

FERRITE SPECIFICATION FOR THE Mu2e 300 kHz AND 4.4 MHz AC DIPOLE MAGNETS

K. P. Harrig, E. Prebys, University of California Davis Physics Dept., Davis, USA,
L. Elementi, C. Jensen, H. Pfeffer, D. Still, I. Terechkine, S. J. Werkema, M. Wong-Squires
Fermilab National Accelerator Laboratory, Batavia, USA

Abstract

The Mu2e experiment at Fermilab will measure the rate for neutrinoless-conversion of negative muons into electrons with never-before-seen precision. This experiment will use a pulsed 8 GeV proton beam with pulses separated by 1.7 μ s. To suppress beam induced backgrounds to this process, a set of dipoles operating at 300 kHz and 4.4 MHz have been developed that will reduce the fraction of out-of-time protons at the level of 10^{-10} or less. Selection of magnetic ferrite material for construction must be carefully considered given the high repetition rate and duty cycle that can lead to excess heating in conventional magnetic material. A model of the electromagnetic and thermal properties of candidate ferrite materials has been constructed. Magnetic permeability, inductance, and power loss were measured at the two operating frequencies in toroidal ferrite samples as well as in the ferrites from which prototype magnets were built. Additionally, the outgassing rates of the ferrite material was measured to determine vacuum compatibility. The outcome of this work is a detailed specification of the electrical and mechanical details of the ferrite material required for this application.

INTRODUCTION

The Mu2e experiment aims to observe conversion to an electron of a muon that has been captured by an aluminium nucleus. This process violates charged lepton flavor number and is forbidden by the standard model. A conclusive result, null or otherwise, would shed light on beyond the standard model physics. The Mu2e collaboration aims to improve on the sensitivity of previous measurements of this process by four orders of magnitude. Specifically, the experiment will measure the ratio of the coherent neutrinoless conversion in the field of a nucleus of a negatively charged muon into an electron to the muon capture process.

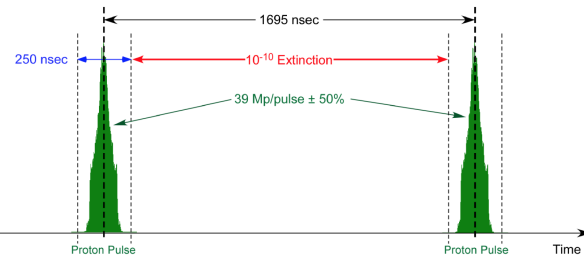


Figure 1: Longitudinal structure of the proton beam after exiting the Delivery Ring [2].

$$R_{\mu e} = \frac{\mu^- + A(Z, N) \rightarrow e^- + A(Z, N)}{\mu^- + A(Z, N) \rightarrow \nu_\mu + A(Z, N)} \quad (1)$$



Figure 2: Fermilab accelerator complex.

The first search for a muon to electron conversion took place in 1955 [1]. However, more recent experiments placed a 90% CL limit on the process of 4.6×10^{-12} , and 7×10^{-13} [1]. A key component to the increase in sensitivity is the longitudinal structure of the proton beam shown in Fig. 1. Specifically, the experiment hopes to achieve $R_e = 6 \times 10^{-17}$ at 90% CL limit. The muons will be created via the decay of pions created by 800 GeV protons impinging on a tungsten target. The out-of-time protons will be eliminated using the extinction system located on the M4 beam line just before the tungsten target. The muons will then be captured on an aluminium nucleus and the resulting electrons will be detected [1]. A diagram of the accelerator complex is shown in Fig. 2. The proton pulses are 250 ns wide and spaced 1.7 μ s apart. Each pulse contains 39×10^6 protons. The experimental signature of the process will include a large background from muons decaying in the orbit of the nucleus before capture can occur.

EXTINCTION

The ratio of out of time protons to total number of protons in a pulse is defined as the extinction. The goal is to obtain a

MC7: Accelerator Technology

T09: Room Temperature Magnets

ratio of 10^{-10} by the time the protons reach the tungsten production target. The extinction is in part accomplished with the formation of the bunches in the Recycler and Delivery Rings.

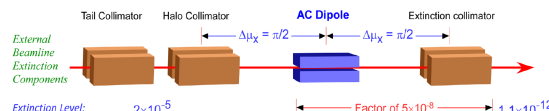


Figure 3: Extinction system consisting of three collimators and two magnets [2].

At the delivery ring the extinction is at the 10^{-5} level. However, the extinction system depicted in Fig. 3 will be responsible for reducing the ratio another five orders of magnitude. The system will involve three collimators and two one meter long AC dipole magnets, that will be referred to going forward as the AC Dipole. The tail collimator will remove the protons scattered by the electrostatic septum upon extraction from the delivery ring. The halo collimators will remove the high amplitude protons (i.e. the protons at the edge of the separatrix in phase space) so that they will not be pushed back into the space of the target by the AC dipole.

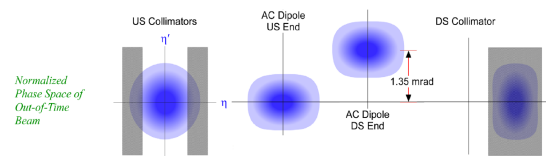


Figure 4: The phase space effects of the extinction system [2].

The extinction collimator will then stop all protons deflected by the AC Dipole. The effects of the extinction system in phase space are shown in Fig. 4. As stated above, the AC Dipole will be responsible for kicking out-of-time beam into the extinction collimator. The requirement for total extinction can be realized in terms of the angular deflection in phase space given by:

$$\Delta\theta = 2\sqrt{\frac{A}{\beta_x\beta\gamma}} \quad (2)$$

This is twice the angular amplitude of the beam admittance A . β_x is the longitudinal betatron function. β and γ take their relativistic definitions. A depiction of this angular distribution in phase space is shown in Fig. 4. The design of the AC dipole was determined by the transmission window, the transmission efficiency for the proton beam and the intensity of the proton pulses.

The AC dipole will be driven by two harmonics: one at 300 kHz and 4.5 MHz. The 300 kHz harmonic is half of the bunch frequency and the 4.5 MHz harmonic is used to maximize the transmission window for the in time protons in the pulse. Figure 5 shows the AC dipole waveform overlaid with proton pulses at the transmission points.

MC7: Accelerator Technology

T09: Room Temperature Magnets

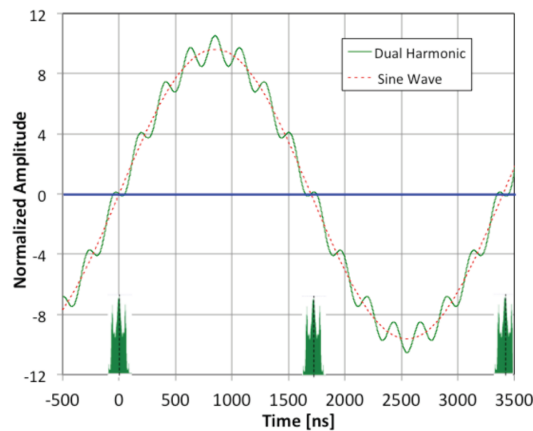


Figure 5: The AC dipole waveform overlaid with proton pulses at the transmission points [3].

Ferrite Characterization

The magnetic material had to be carefully considered due to the extremely high repetition rate. A soft NiZn ferrite was chosen as the material for its low coercivity and high curie temperature, resistivity and magnetic permeability. The magnetic flux density, B , and the magnetizing field, H , are related by the magnetic permeability:

$$B = \mu\mu_0H \quad (3)$$

Where μ is the magnetic permeability of the ferrite material and μ_0 is the permeability of free space. $\mu = \mu' - \mu''$ is a complex number that depends on frequency and excitation and is related to power loss:

$$Q = \frac{\mu'}{\mu''} \quad (4)$$

where Q is the quality factor that in general relates the energy stored to the average power loss. Ferrite losses depend on many factors but losses due to material heating can be contributed to eddy currents in the material. However, this behavior can be unpredictable, especially at higher frequencies and excitation level. For this reason there is really no way of predicting the power and heating in the material, so a rigorous characterization methodology had to be developed and tested.

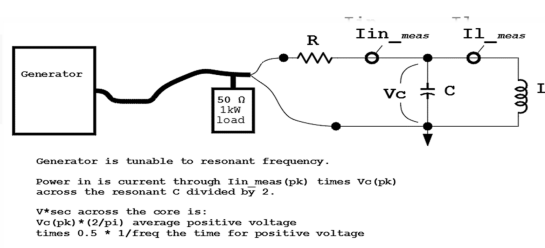


Figure 6: Circuit diagram for ferrite characterization.

Experimental Setup Figure 6 describes the general circuit diagram used to measure the power loss in the ferrite material. It consists of a capacitor bank connected in parallel to the ferrite bricks that are arranged as shown in Fig. 7 with a three turn copper coil. The resistor is used to reduce noise from the power amplifier. The 3500 W power amplifier and a signal generator were used to excite the ferrites.



Figure 7: Overview of circuit setup for ferrite characterization. A voltage, and two current probes in conjunction with an oscilloscope are used to measure the voltage across the capacitor bank, the current through the copper coil and the current into the circuit respectively.

Experimental Setup and Methodology The circuit can be made to resonate at the two relevant frequencies (300 kHz and 4.5 MHz) by adjusting the capacitance:

$$\omega_0 = \frac{1}{\sqrt{LC}} \quad (5)$$

The power loss is calculated using the input current and the voltage. A point by point integration gives the power as a function of excitation. The excitation is calculated using the following formula:

$$B = \frac{2NI_{ind-peak}}{\mu_0 g} \quad (6)$$

Where N is the number of turns in the copper coil, $I_{ind-peak}$ is the current in the copper coil and g is the gap between the ferries which was 1.8 cm.

Results Figures 8 and 9 show the losses as a function of excitation field at each frequency.

CONCLUSION

The power losses were found to be reasonable for the given field requirements and out of the over 300 bricks that will be used to make up the actual magnets, about 7% have

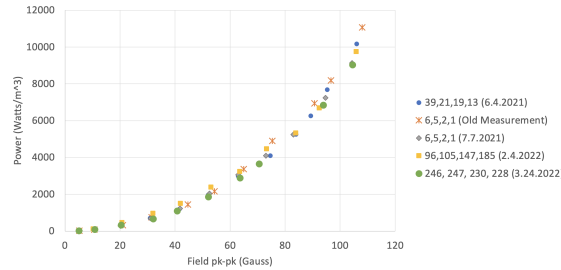


Figure 8: Losses at 300 kHz, with 26.4 nF capacitance. The bricks were measured in groups of four and are labeled by their manufacturing number and date measured. At the field strength required by the magnet the ferrites will experience losses $\sim 15.000 \text{ W/m}^3$.

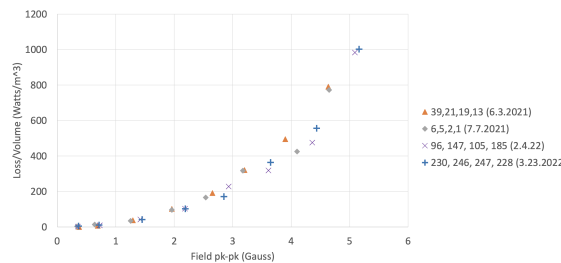


Figure 9: Losses at 4.4 MHz, with 68 pF capacitance. The bricks were measured in groups of four and are labeled by their manufacturing number and date measured. At the field strength required by the magnet the ferrites will experience losses $\sim 1.000 \text{ W/m}^3$.

been characterized. Future work will include characterizing a larger percentage of the bricks as well as mechanically assessing the mating surfaces.

REFERENCES

- [1] L. Bartoszek and *et al.*, “Mu2e Technical Design Report”, 2014. doi:10.48550/arXiv.1501.05241
- [2] S. Werkema, “Mu2e Proton Beam Longitudinal Structure”, Mu2e-doc-2771, 2014. <http://mu2e-docdb.fnal.gov/>.
- [3] E. Prebys, ed., “Extinction in the Mu2e Beam Line”, *AIP Conf. Proc.*, vol. 1222, p. 415, 2010. doi.org/10.1063/1.3399357